Hypersonic Flow Diagnostic Studies in a Large Arc-Heated Wind Tunnel

JAMES L. FOLCK* AND RICHARD T. SMITH†
Air Force Flight Dynamics Laboratory, Wright-Patterson Air Force Base, Ohio

This study consisted of the experimental investigation of test flow in an arc-heated hypersonic wind tunnel. These tests utilized a high-voltage d.c. arc heater which operated at input powers in excess of 50 Mw and provided reservoir pressures ranging from 100 to 1500 psi and bulk enthalpies from 1500 to 4000 Btu/lb. Local freestream measurements of Pitot pressure, mass flux, stagnation point heat-transfer rate, and wall static pressures were obtained at the exit of a nominal 2-ft-diam conical nozzle. Stagnation enthalpy profiles at the nozzle exit became peaked at high stagnation pressures. From these data, centerline enthalpies as high as 6500 Btu/lb were indicated in the flow. Selective comparisons between theory and experiment are presented. At a reservoir enthalpy of approximately 2500 Btu/lb and for stagnation pressures in excess of 500 psi, the expanded flow data were in good agreement with equilibrium expansion theory. However, below 500 psi, the data compared more closely with nonequilibrium theory with the flow frozen downstream of the nozzle throat.

Nomenclature

A = area, ft²
A^* = throat area, ft²
C_P = specific heat at constant pressure
E = voltage
H = enthalpy, Btu/lb
I = current, amperes
Le = Lewis number
$\dot{m}$ = water flow rate, lb/sec
P = pressure, psia
Pr = Prandtl number
P_{T_2} = Pitot pressure, mm Hg
$\dot{q}$ = heat-transfer rate, Btu/ft²-sec
R,r = radius
ΔT = temperature change
u = velocity, fps
L = characteristic length
δ^* = boundary-layer displacement thickness
η = efficiency, %
μ = viscosity
ρ = density, lb/ft³
$\dot{\omega}$ = air mass flow rate, lb/sec

Subscripts

d = dissociation
esf = equilibrium sonic flow
$F\&R$ = Fay and Riddell equation
HB = heat balance
H_2O = water property
0 = stagnation conditions
r = reference conditions
s = local stagnation conditions
w = conditions at wall
∞ = freestream conditions

1. Introduction

ARC-heated hypersonic wind tunnels play an important role in today's aerospace technology. These facilities are required to study aerodynamic heating and ablation characteristics associated with hypersonic cruise and re-entry vehicles. This type of an investigation requires an extreme hyperthermal environmental facility capable of operating on a continuous basis. The arc heater is one of the best available means for establishing the required reservoir conditions. However, most arc heaters have some inherent characteristics which for certain operating conditions can result in large radial temperature gradients across the jet.

Also, because of high stagnation temperatures produced in the arc chamber, the vibrational energy modes of the gas molecules become excited and an appreciable amount of dissociation occurs. As the gas is expanded through a nozzle, the rapid changes in temperature and density are sufficiently rapid that the recombination and vibration de-excitation reaction processes cannot equilibrate. The resultant thermal and chemical nonequilibrium gas state is characterized by a reduction in the velocity, static pressure, and temperature as compared to an equilibrium expansion. Experiments[1-3] have shown that an equilibrium expansion of a high-temperature gas can only be achieved for a very restricted range of reservoir conditions. Thus, a nonequilibrium expansion process must be considered for the general case. Theoretical studies[1,4-6] of a nonequilibrium expansion process have been made using an inviscid, one-dimensional, chemically reacting gas model. However, to date, no successful attempt has been made in coupling the nonequilibrium expansion with a realistic boundary-layer calculation. Therefore, until this is accomplished, these programs cannot be used to predict arc heater-nozzle performance. Thus, the important test section flow parameters must be experimentally determined. Several plasma diagnostic studies have been reported,[7-10] yet the study presented here is one of the most complete calibrations of an arc-heated hypersonic wind tunnel which has been accomplished to date. Local freestream measurements of Pitot pressure, mass flux, stagnation point heat-transfer rate, and wall static pressure have been made and selective comparisons between theory and experiment are presented.

2. Description of Equipment and Instrumentation

This facility is the Air Force Flight Dynamics Laboratory 50 Mw Electrogasdynamics Facility. This wind tunnel, described in Ref. 11, is of a continuous flow type utilizing high-pressure dry air, heated by a high power, high-voltage arc heater, and exhausted through several stages of vacuum pumps. The arc heater shown in Fig. 1 consists of two coaxial tubular electrodes separated by an electrically insulated air inlet chamber. Air is injected tangentially into the heater

Received May 14, 1969; revision received February 2, 1970.
* Aerospace Engineer, Thermomechanics Branch.
† Technical Manager for Test Operations, Thermomechanics Branch; presently, Senior Engineer, Arnold Research Organization, Arnold Engineering Development Center, Tullahoma, Tenn.

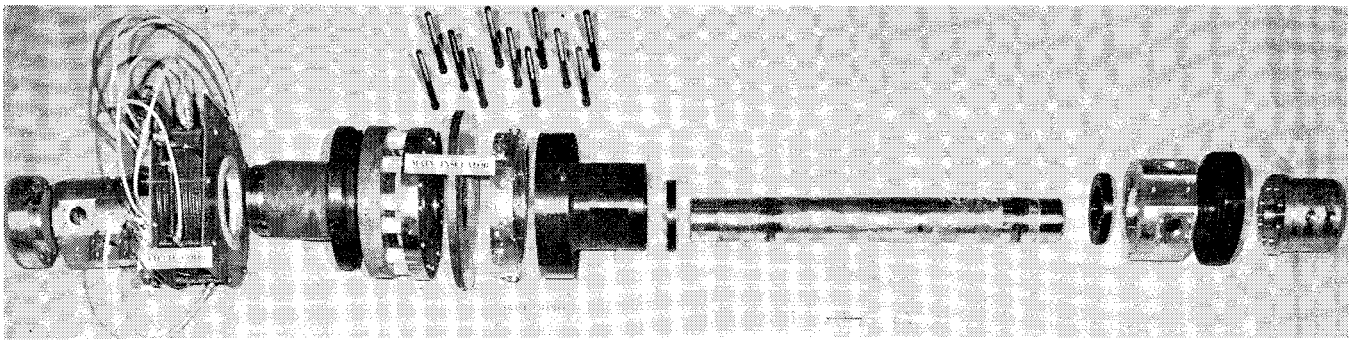

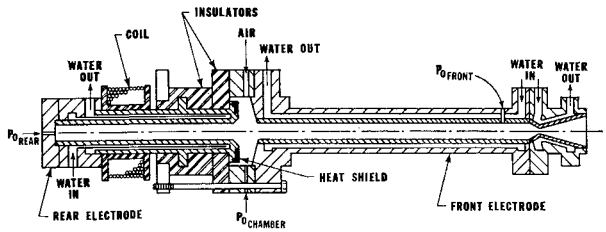

Fig. 1 High-pressure arc heater.

which induces a vortex flow to stabilize the arc and rotate the arc attachment points. The arc heated flow was expanded through a 16° (included angle) conical nozzle with a 1-in.-diam throat and 25.2-in. exit diameter. All wind-tunnel components subjected to critical heating rates are protected by high-pressure, high-velocity, back side water cooling.

The primary flow diagnostic probes used in this investigation consisted of a total pressure probe, a mass flux probe, and a stagnation point heat transfer probe. These probes have an external diameter of 1 in. and are approximately 12 in. long. Details of the design of these probes are described in detail in Ref. 12. The mass flux probe is a sharp lipped aspirating type probe designed to fully capture a small tube of the freestream flow which is pumped through a calibrated orifice. Knowing the inlet area of the probe allows one to determine the local mass flux (ρu). In order to measure the Pitot pressure, a valve was closed in the aspirating flow line causing the flow to stagnate so that consecutive measurements of ρu and P_{T_2} could be made. The stagnation point heat-transfer probe consists of a small thermally insulated copper slug located at the stagnation region of the nose and cooled by high-velocity water. The steady-state heat input to the nose cap, determined from the water flow rate and temperature rise, is converted to stagnation point heating rate by applying the proper constants to account for distribution effects. A small Pitot pressure probe with an external diameter of 0.0625 in. was also used for detailed boundary-layer measurements.

The primary data acquisition equipment for these tests consisted of an Ambilog hybrid (analog-digital) data processor that allowed on-line data reduction and computation.

3. Experimental Procedure and Data Presentation

3.1 General Test Procedure

The arc heater was started and the nozzle flow was established. The arc voltage and current were then adjusted to give the desired test conditions.

The probe was then inserted into the flow and positioned radially across the jet by manual control of the hydraulic drive control system. The surveys were made using a step-pause technique to eliminate the possibility of errors from slow time response instrumentation. At each test point, the data acquisition system was activated and all data channels, including the arc heater parameters, were simultaneously recorded, computed, and stored on magnetic tape. Several test conditions could be obtained during a run by resetting the arc-heater conditions and repeating the test sequence. Typical continuous run duration for this test series was from 10 to 30 min. During the test, periodic instrument checks and calibrations insured the accuracy of the measured value of the various parameters.

3.2 Arc Heater Performance

These flow studies, which are reported in detail in Refs. 13 and 14, were conducted in conjunction with an extensive facility calibration and arc-heater development program. A typical arc-heater performance curve is presented in Fig. 2. In this type of heater the arc length and attachment points are not fixed. The arc length and operating voltage increase with the air mass flow and reservoir pressure. Consequently, as the heater pressure is increased, the downstream arc termination approaches and can blow through the nozzle throat. The initial runs were made with a 45-in.-long front electrode installed in the heater. For this electrode length, the arc would blow through the throat and terminate downstream of the nozzle wall when the arc chamber pressure exceeded approximately 500 psi. This caused a highly ionized core at the flow centerline. To alleviate this condition, the electrode length was increased to 72 in. and finally to 96 in. The increased length permitted heater operation at successively higher reser-

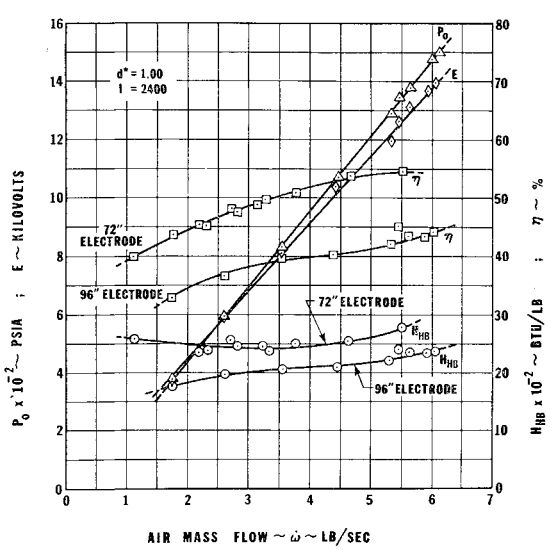

Fig. 2 Typical arc-heater performance characteristics.

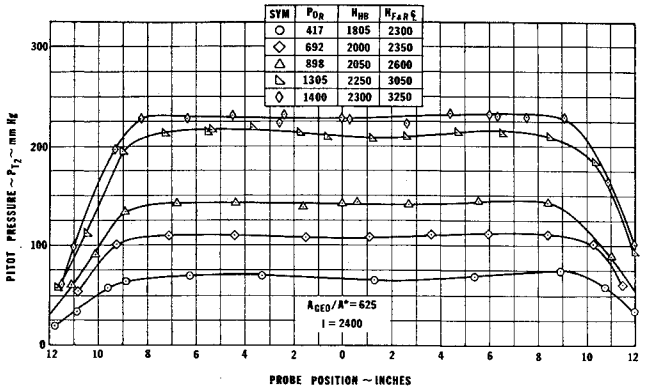

Fig. 3 Typical Pitot pressure profiles with 96-in. electrode.

voir pressures and improved the flow uniformity at the nozzle exit. The heater efficiency dropped slightly, but generally ranged from 35% to 60% for all the operating conditions and configurations tested. The majority of the test program was accomplished using a 1-in.-diam throat which operated at reservoir pressures from 300 to 1500 psi and input power to 35 Mw. Using a 2-in.-diam throat restricted the pressure range from 100 to 500 psi, but permitted operation at higher enthalpy levels with input power to 51.7 Mw. Bulk or heat balance enthalpies ranging from 1500 Btu/lb to 4000 Btu/lb were obtained.

3.3 Nozzle Exit Measurements

Nozzle exit surveys and centerline measurements of the Pitot pressure, mass flux, stagnation point heat-transfer rate, and wall static pressure were obtained for all available reservoir conditions. Discussion of the centerline Pitot pressure measurement and wall static pressure data will be reserved for a following section. The radial flow surveys made during these tests were of major importance in the flowfield calibration. These surveys show that arc heater configuration, particularly the front electrode length, exhibited a strong influence on the nozzle exit flow uniformity.

Pitot pressure—mass flux surveys

Radial Pitot pressure and mass flux profile measurements were obtained for numerous reservoir conditions for all the arc-heater configurations. Typical survey data, given in Figs. 3 and 4, for the 96-in. electrode configuration show that these profiles were very uniform across the inviscid core for stagnation pressures to 100 atm. Pitot pressure surveys made with the shorter arc heater configuration showed a tendency to dip slightly toward the nozzle centerline particularly when operating the heater at high pressures or high currents. However, these effects were minimal and all the surveys across the core

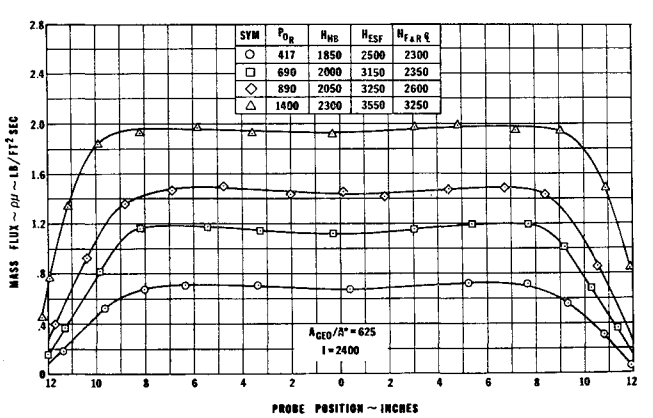

Fig. 4 Mass flux profiles, with 96-in. electrode.

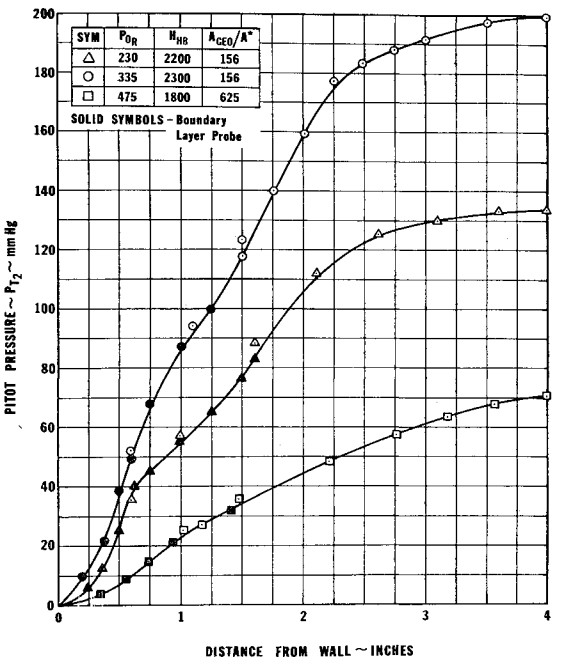

Fig. 5 Boundary-layer Pitot pressure profiles.

flow were flat to within 5% of the centerline values for all the arc heater conditions and configurations tested.

Detailed Pitot pressure profiles in the boundary layer were obtained for several operating conditions and are shown in Fig. 5. The small water cooled Pitot probe was used for the measurements near the wall to improve the resolution and positioning accuracy.

Stagnation-point heat-transfer data

Stagnation-point heat-transfer rate profiles and centerline measurements were made for numerous arc-heater operating conditions. On the first few runs made with the probe, it was noted that a black copper oxide coating would form over the copper sensing slug as well as remaining probe surfaces. Several studies[15,16] have shown that surface oxidation can make the wall non-catalytic to atom recombination and may cause a significant reduction of the heat-transfer rate. However, the analysis in the next section shows that the majority of the dissociation energy was recovered.

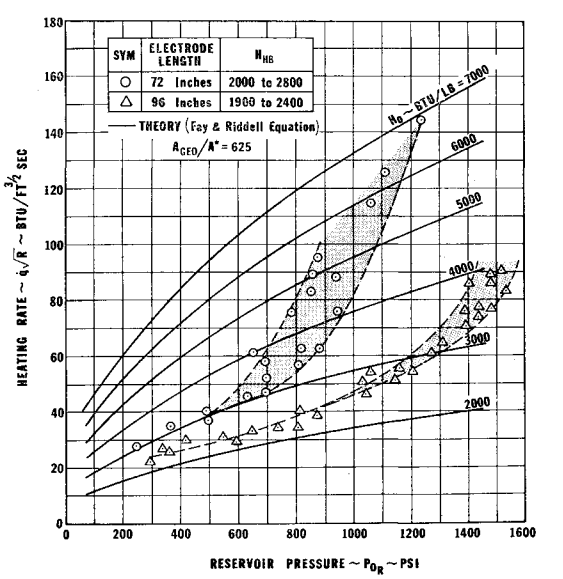

Fig. 6 Typical centerline stagnation-point heat-transfer rate. Measurements with the 72-in. and 96 in. electrodes.

Initially, the centerline measurements of the heat-transfer rate shown in Fig. 6 were difficult to interpret at the high-pressure conditions due to the data scatter and inconsistent trends. These data were brought into proper perspective by examining the complete radial profiles at various operating conditions. The effects of heater pressure on the profile shape for the 96-in. electrode configuration is shown in Fig. 7. Note that the arc heater with the long electrode could be operated to pressures of 1000 psi with uniform profiles across the core.

3.4 Total Enthalpy Measurements

The total enthalpy of the gas is one of the most important test parameters to be duplicated and therefore, several methods of measuring it were employed.

Heat balance method

An energy balance of the arc heater and nozzle can be made by measuring the electric power input to the heater and the energy loss to the cooling water. The d.c. power to the arc heater was determined by continuously monitoring the operating voltage and current. The air mass flow rate was measured with an unchoked calibrated orifice located upstream of the heater. The water flow rates and the temperature rise of the cooling water to the electrodes and swirl chambers were used to determine the energy loss in the heater, from which the heater efficiency and heat balance enthalpy were calculated. The losses to the throat were a maximum of 2.5% of the heater input power and were not included in the heat balance enthalpy calculations. Combining the heater energy balance with the air flow rate gives the bulk or heat balance enthalpy

$$H_{HB} = [EI - (\dot{m}C_P\Delta T)_{H_2O}]/\dot{\omega} \qquad (3.1)$$

The heat balance enthalpy being a bulk measurement is not representative of the true centerline enthalpy because of the nozzle boundary layer and the incomplete heat diffusion from the arc.

Equilibrium sonic flow method

The total enthalpy of the flow can also be obtained from the throat area, air mass flow rate, and stagnation pressure by using the equilibrium sonic flow theory. An empirical expression of this type formulated by Winovich[17] is given by

$$H_{esf} = (280A^*P_0/\dot{\omega})^{2.519} \qquad (3.2)$$

The assumption inherent in this equation is that the flow can be represented by a uniform one-dimensional equilibrium flow through the throat with a discharge coefficient of one. The arc heater geometry and flow pattern and gas chemistry must be critically analyzed to determine the applicability in each particular case.

The equilibrium sonic flow enthalpy was calculated for the present test conditions and compared with the enthalpy based on the heat transfer probe and the heat balance enthalpy. This comparison shows that the sonic flow enthalpy calculated from the above equation was as much as 30% higher than the centerline heat-transfer probe enthalpy and approximately 50% higher than the heat balance enthalpy. The higher enthalpy is believed to be caused by the reduction of the effective throat area due to a strong swirl flow in the heater. Several cold blow tests were made blowing air through the heater with and without the swirl injectors installed. The heater pressure and air mass flow rate were recorded for each configuration. The swirl flow in the heater was found to reduce the mass flow rate by approximately 20% for fixed heater stagnation pressures. Thus, the swirl flow reduces the effective throat size for ambient air temperatures. The same effects should be present with the arc heater operating, but the magnitude could not be directly measured since the swirl is required to stabilize the arc during normal operation.

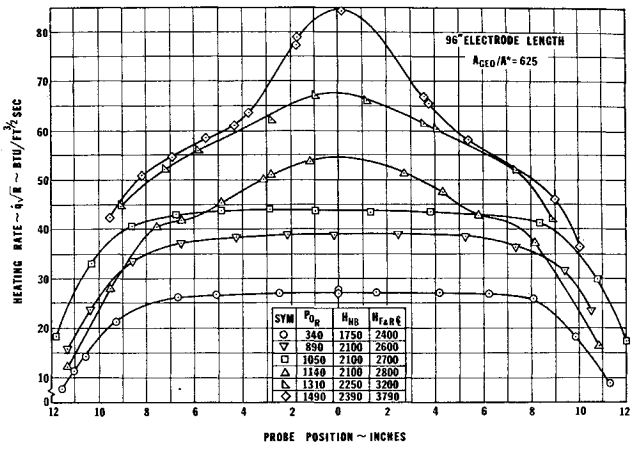

Fig. 7 Stagnation-point heat-transfer rate profiles showing the effect of pressure on flow uniformity with 96-in. electrode.

Since the effective throat diameter appears in the equilibrium sonic flow equation to a power of about 5, a small error in this parameter will give gross errors in the enthalpy calculated by this equation. Thus, any correlation between this method and the true stagnation enthalpy is strictly fortuitous and should not be used for a vortex stabilized arc heater.

Stagnation-point heating rate method

The total enthalpy can also be calculated from measurements of the stagnation-point heat-transfer rate and Pitot pressure by using a theoretical equation relating these quantities. The theoretical determination of the aerodynamic heating rates for high enthalpy flows is complicated due to the large amount of dissociation energy that can become frozen in the flow. If complete recombination of the atoms does not occur the measured heating rate and consequently the enthalpy can be considerably reduced. Total enthalpy of the flow was determined by combining the local measurements of Pitot pressure and heat-transfer rates with equilibrium heating rate theory. The theoretical equation of Fay and Riddell[18] relating the heat-transfer rate and the total enthalpy with the assumption of a fully catalytic wall was used in the calculations

$$H_{F\&R} = h_w + \frac{\dot{q}(R)^{1/2}}{0.906P_r^{-0.6}(\rho\mu)_w^{0.1}(\rho\mu)_s^{0.4}[1 + (Le^{0.52} - 1)h_d/H_0](P_{T_2}/\rho_{T_2})^{0.25}} \qquad (3.3)$$

The transport properties were evaluated using the real gas approximations of Hansen.[19] In addition to the gas chemistry and wall catalytic effects, studies reported in Ref. 20 indicate that the heating rates can also be influenced by free-stream turbulence. These effects are not fully understood and the best analysis available cannot be used to obtain quantitative results. Thus, when the stagnation-point heating rate method is used to determine the flow total enthalpy, an independent measurement should be made with which to corroborate the results.

Discussion of results

The total enthalpy profiles were highly peaked for some operating conditions and follow the same trends as the heat-transfer distributions due to the uniform pressure profiles. Enthalpy profiles shown in Fig. 8 for the 72-in. electrode configuration show that peaking can produce centerline enthalpies almost three times higher than heat balance values. Enthalpy profiles for the 96-in. electrode also shown in Fig. 8 were flat up to a pressure of approximately 1000 psi. Further in-

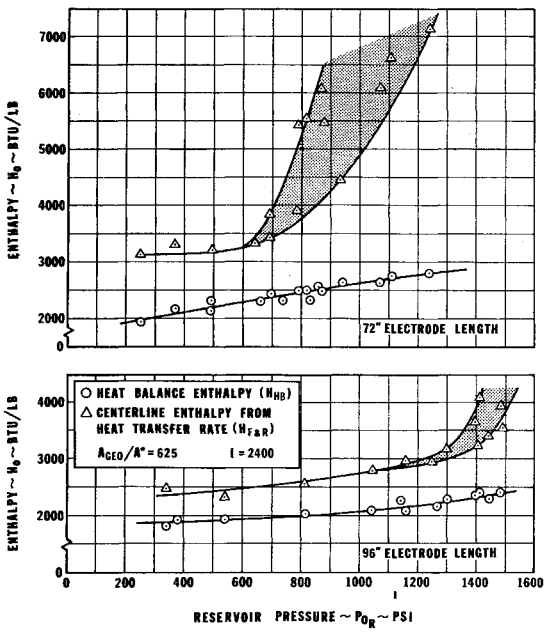

Fig. 8 Total enthalpy profiles showing the effects of pressure and operating current.

creases in pressure causes the enthalpy profile to peak near the center of the flow. The maximum increase in centerline enthalpy for this arc heater configuration was 40% above the heat balance enthalpy. The peaked enthalpy profiles did not follow a consistent trend as is exemplified by the surveys at 1140 psi and 1310 psi. Thus, duplicating the arc heater geometry and pressure in the operating range where peaking occurs will not insure repeatable centerline conditions.

Centerline and heat balance enthalpy measurements are summarized in Fig. 9 and show the effects of pressure and front electrode length. The data for the 72-in. electrode show that the peaking starts at approximately 600 psi and the centerline enthalpy is scattered depending on many factors including rear coil position and electrode surface condition. The centerline enthalpy peaking for the 96-in. electrode did not become significant until pressures exceeded 1000 psi. Below this pressure the data could be consistently repeated to within 5% or less.

The enthalpy peaking is most likely caused by the arc approaching the nozzle throat and not allowing sufficient mixing

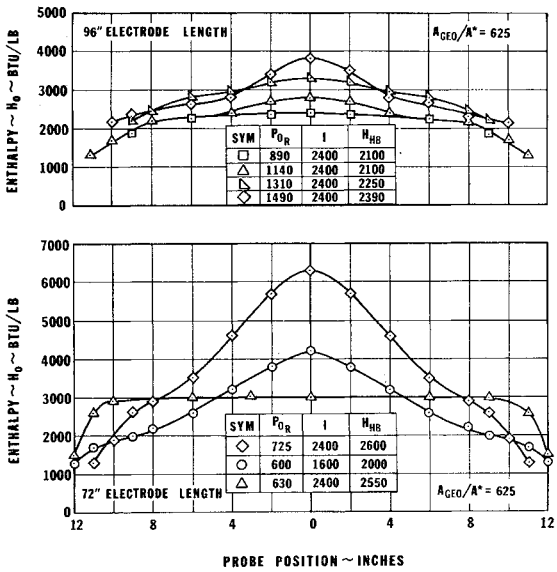

Fig. 9 Total enthalpy measurements with the 72-in. and 96-in. electrodes.

Table 1 Comparison of Enthalpy Measurement Techniques

Electrode length, in.	P_0, atm	I, amp	Power, Mw	η, %	$H_{F\&R}$, Btu/lb	H_{HB}, Btu/lb	$\langle H_{F\&R} \rangle$, Btu/lb
96	60.5	2400	19.2	0.40	2410	2080	2150
96	101.5	2400	32.2	0.48	3790	2390	2160
45	29.2	4000	11.0	0.51	4930	3350	3340
45	42.9	3200	18.9	0.45	4480	3380	3210

length for the hot gas. The peaking starts when the arc termination is about 10 electrode diameters from the throat and continues until the arc blows through the nozzle throat. The longer electrode configurations resulted in a more uniform temperature distribution and subsequently reduced the centerline enthalpy. However, this increased length reduced the data scatter and increased the pressure capability without a large decrease in the heat balance enthalpy. The over-all effect of the increased electrode length was to significantly improve the flow uniformity and the arc heater high-pressure capability.

The enthalpy calculated from the heat-transfer Pitot probe measurements and the heat balance enthalpy were found to be consistent. The enthalpy surveys from the heat-transfer probe can be combined with the mass flux profiles to give an average or bulk enthalpy defined by

$$\langle H \rangle = \frac{2\pi}{\dot{\omega}} \int_0^R H(\rho u) r dr \tag{3.4}$$

This equation was numerically integrated for several varied profile shapes and operating conditions with the results summarized in Table 1. The favorable agreement between the heat balance enthalpy and the integrated enthalpy profiles based on the heating rate and Pitot pressure measurements shows that the assumptions of fully catalytic wall and equilibrium heating rate theory are valid for the range of conditions tested.

4. Comparison of Experimental Results with Theory

4.1 Theoretical Analysis

In order to compare the experimental results of this investigation with theoretical predictions, several calculations were performed with the aid of a 7094 computer using a real gas nozzle expansion program. The flow model for these calculations tailored after the work of Yoshikawa and Katzen[21] assumes steady-state, one-dimensional flow that is expanded from a given set of reservoir conditions (H_0, P_0) either isentropically or in a predetermined chemically frozen state. The thermodynamic properties were obtained using the Arnold Engineering Development Center (AEDC) WRKHAT computer program developed by Lewis and Burgers.[22] The frozen flow calculations were made assuming the chemical composition of the gas fixed at the nozzle throat.

The effects of the boundary-layer displacement was included in the analysis by using an empirical equation for calculating the displacement thickness. An iteration routine was used, alternately calculating the expansion properties and then the displacement thickness. The assumed inviscid exit diameter was corrected using the calculated value of the displacement thickness and the expansion was then recalculated. This process was continued until convergence was obtained.

4.2 Boundary-Layer Thickness Determination

The boundary-layer displacement thickness was calculated in this program using an empirical expression developed by

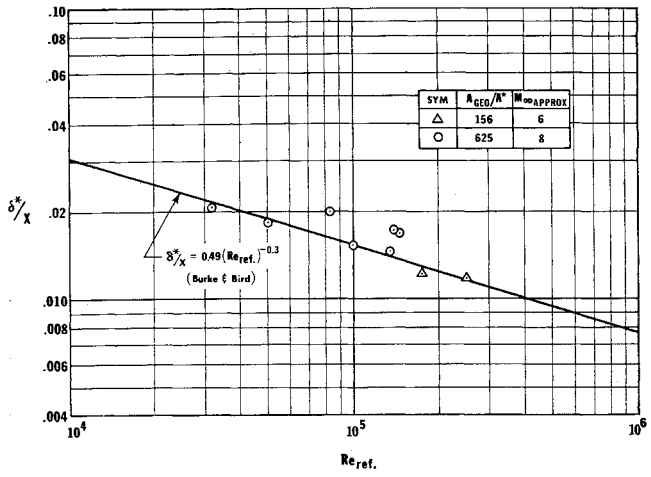

Fig. 10 Correlation of displacement thickness data.

Burke and Bird[23]:

$$\delta^* = 0.49L(\rho_r u L/\mu_r)^{-0.3} \qquad (4.1)$$

where the density and viscosity were evaluated at the Eckert reference enthalpy[24] given by

$$H_r = 0.22H_0 + 0.5H_w + 0.28H_\infty \qquad (4.2)$$

Several more recent formulas and techniques for calculating displacement thicknesses have been formulated[6,25] in an attempt to provide a better curve fit over a wider range of test conditions. However, the validity of this boundary-layer correction was checked experimentally by numerically integrating several mass flux profiles to obtain the boundary-layer displacement thicknesses at various operating conditions. Comparing the results of these integrations with the Burke and Bird equation in Fig. 10 shows that this equation is adequate in the Mach number and Reynolds number ranges covered in these tests. The scatter of some of these data points can be attributed to the relatively large mass flux probe and the large spacing between data points. These data points were typically one half inch apart in a 4-in.-thick boundary layer.

4.3 Correlation of Nozzle Exit Pressures

The nozzle expansion program was run for reservoir conditions consisting of enthalpies ranging from 2000 to 4000 Btu/lb and stagnation pressures from 200 to 1400 psi. Expansions based on these assumed reservoir conditions and nozzle geometries were calculated for equilibrium and frozen flow models. The results are compared with Pitot pressure and static pressure measurements in Figs. 11 and 12.

Pitot pressure calculations are shown to be relatively insensitive to the flow model employed and therefore cannot be used to determine the chemical state of the gas. Centerline Pitot pressure measurements shown in Fig. 11 correlated well with the reservoir pressure and were independent of all other operating parameters. A straight line fairing through these data was made with a mean deviation of less than 1%. Also, it should be noted that since the impact pressure is insensitive to the state of the gas, this is also a measure of the effective area ratio of the nozzle and provides an independent check on the displacement thickness calculations.

It has been shown that the effect of the swirl flow in the arc heater can cause significant errors in calculating the mass flow rate and flow enthalpy using one-dimensional sonic flow theory. This, however, has little effect on the test section flow. Estimates of the radial distribution of the test section flow swirl angle have been made by measuring the pressure differentials on a multiorifice hemispherical probe. From

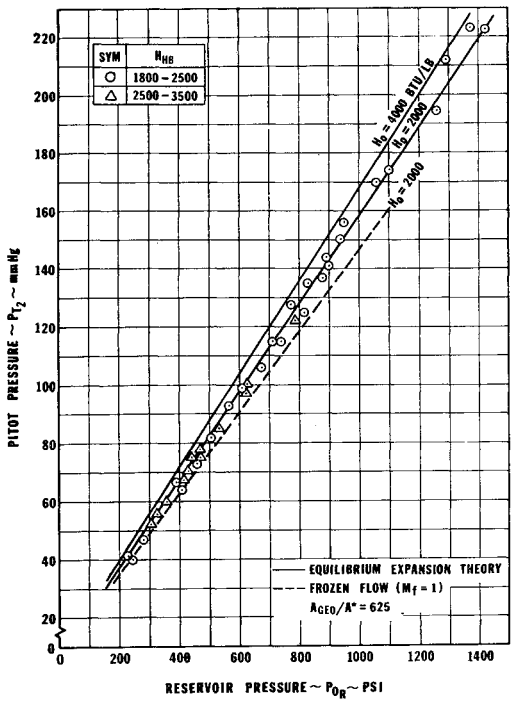

Fig. 11 Comparison of typical centerline Pitot pressure with theory.

these tests it was concluded that the flow swirl angle in the test section was negligible.

Departures from equilibrium in the expansion process can cause large differences in nozzle exit static pressures. Wall pressures were measured over a range of reservoir pressures and are compared with theory in Fig. 12. In the pressure range from 100 to 500 psi, the data fall between the equilibrium and frozen flow theory. Since the chemistry was assumed frozen at the throat, this would indicate that the nonequilibrium starting point is slightly downstream of the throat. No attempt was made to adjust the nonequilibrium starting point as is usually employed in this type analysis; however, this technique would bring the data and theory into closer agreement. For reservoir pressures in excess of 500 psi, the nozzle exit static pressures were in good agreement with

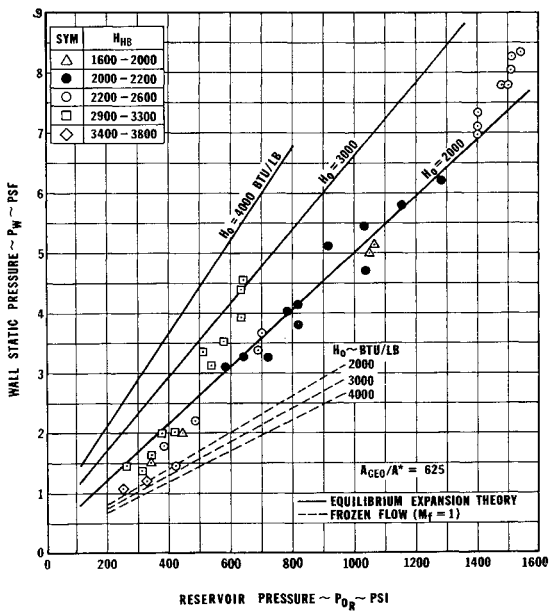

Fig. 12 Comparison of nozzle wall static pressure measurements with theory.

equilibrium expansion theory. Shock tunnel experiments reported by Nagamatsu[2,3] gave almost identical results.

5. Conclusions

These investigations have shown that for the range of conditions tested, the standard hypersonic flow diagnostic measurements of pressure, mass flux and heat-transfer rate are adequate for determining the flow uniformity and the gross thermochemical state of the gas. The radial flow surveys were of major importance in assessing the flow quality and therefore, must be included in the flowfield calibration of any arc heated wind tunnel. The Pitot pressure and mass flux measurements alone can give an inaccurate picture of the flow uniformity. These data must be accompanied by a local measurement of the stream temperature or enthalpy to completely describe the flowfield.

From the three independent enthalpy measurement techniques which were evaluated, it can be concluded that the heating rate method can be successfully used in a high pressure arc heated wind tunnel to determine the local total enthalpy of the expanded flow. The sonic throat method of enthalpy determination was critically analyzed for a vortex stabilized arc heater and shown to be susceptible to large errors due to the strong swirl flow which exists at the throat. The experimental expanded flow data were found to be in good agreement with one-dimensional real gas flow analysis when the appropriate reservoir conditions are used and boundary-layer corrections are applied. Using the heat balance enthalpy and arc-heater pressure as the reservoir conditions, the nozzle exit pressure correlated even when the enthalpy profiles were highly peaked.

For reservoir enthalpies from 2000 to 2500 Btu/lb and heater pressures in excess of 500 psi, the expanded flow data were in good agreement with equilibrium expansion theory. The nozzle static pressures exhibited nonequilibrium expansion characteristics for reservoir pressure less than 500 psi.

Although the peaked enthalpy distribution is not desirable for most aerodynamic type test programs, it may be advantageous for some blunt body aerodynamic heating tests. In this operating mode, centerline stagnation region heat-transfer rates three times higher than normal can be achieved. This severe peaking can be suppressed by proper selection of the front electrode length. Thus, before meaningful aerodynamic and aerothermodynamic testing can be accomplished in arc heated hypersonic facilities, the many problems associated with the arc heater operation, flow diagnostics and the effects of gas chemistry must be carefully analyzed to insure proper simulation of the flight environment.

References

[1] Zonars, D., "Nonequilibrium Regime of Airflows in Contoured Nozzles: Theory and Experiment," *AIAA Journal*, Vol. 6, No. 1, Jan. 1967, pp. 57–63.

[2] Nagamatsu, H. T., Workman, J. B., and Sheer, R. E., "Hypersonic Nozzle Expansion of Air with Atom Recombination Present," *Journal of the Aerospace Sciences*, Vol. 28, No. 11, Nov. 1961, pp. 833–837.

[3] Nagamatsu, H. T. and Sheer, R. E., "Vibrational Relaxation and Recombination of Nitrogen and Air in Hypersonic Nozzle Flows," *AIAA Journal*, Vol. 3, No. 8, Aug. 1965, pp. 1386–1391.

[4] Lordi, J. A. and Mates, R. E., "Nonequilibrium Expansions of High Enthalpy Airflows," ARL-64-206, Nov. 1965, Aerospace Research Lab.

[5] Dresser, H. S., French, E. P., and Webb, H. G., "Computer Program for One-Dimensional Nonequilibrium Reacting Gas Flow," TR-67-75, Aug. 1967, Air Force Flight Dynamics Lab.

[6] Burke, A. F. and Wallace, J. E., "Aerothermodynamic Consequences of Nozzle Nonequilibrium," AEDC-TR-66-47, Feb. 1966, Arnold Engineering Development Center.

[7] Van Camp, W. M. et al., "Study of Arc-Jet Propulsion Devices," CR-54691, March 1966, NASA.

[8] Potter, J. L. et al., "Gasdynamic Diagnosis of High-Speed Flows Expanded from Plasma States," AEDC-TDR-63-241, Nov. 1963, Arnold Engineering Development Center.

[9] Witte, A., Kubota, T., and Lees, L., "Experimental Investigation of a Highly Ionized Arc-Heated Supersonic Free Jet," AIAA Paper 68-135, New York, 1968.

[10] Pope, R. B., "Measurements of Enthalpy in Low-Density Arc-Heated Flows," *AIAA Journal*, Vol. 6, No. 1, Jan. 1968, pp. 103–110.

[11] "Fifty-Megawatt Electrogasdynamics Facility," April 1967, Air Force Flight Dynamics Lab.

[12] Huber, F. J. A., "Probes for Measuring Mass Flux, Stagnation Point Heating, and Total Enthalpy of High Temperature Hypersonic Gas Flows," AIAA Paper 66-750, Los Angeles, Calif., 1966.

[13] Smith, R. T. and Folck, J. L., "Operating Characteristics of a Multi-Megawatt Arc Heater used with the AF Flight Dynamics Laboratory 50-Megawatt," TR-69-6, 1969, Air Force Flight Dynamics Lab.

[14] Folck, J. L. and Smith, R. T., "Calibration of the AF Flight Dynamics Laboratory 50-Megawatt Arc Heated Hypersonic Wind Tunnel with a Two-Foot Nozzle," TR-69-36, Aug. 1969, Air Force Flight Dynamics Lab.

[15] Goulard, R., "On Catalytic Recombination Rates in Hypersonic Stagnation Heat Transfer," *Jet Propulsion*, Vol. 28, 1958, pp. 737–745.

[16] Pope, R. B., "Stagnation Point Convective Heat Transfer in Frozen Boundary Layers," *AIAA Journal*, Vol. 6, No. 4, April 1968, pp. 619–626.

[17] Winovich, W., "On the Equilibrium Sonic-Flow Method for Evaluating Electric-Arc Air-Heated Performance," D-2132, March 1964, NASA.

[18] Fay, J. A. and Riddell, F. R., "Theory of Stagnation Point Heat Transfer in Dissociated Air," *Journal of the Aerospace Sciences*, Vol. 25, No. 2, Feb. 1958, pp. 73–85.

[19] Hansen, C. F., "Approximations for the Thermodynamic and Transport Properties of High-Temperature Air," TR R-50, 1959, NASA.

[20] Weeks, T. M., "Influence of Free Stream Turbulence on Hypersonic Stagnation Zone Heating," AIAA Paper 69-167, New York, 1969.

[21] Yoshikawa, K. K. and Katzen, E. D., "Charts for Air Flow Properties in Equilibrium and Frozen Flows in Hypervelocity Nozzles," TN D-693, April 1961, NASA.

[22] Lewis, C. H. and Burgess, E. G., "Empirical Equations for the Thermodynamic Properties of Air and Nitrogen to 15,000°K," AEDC-TR-63-138, July 1963, Arnold Engineering Development Center.

[23] Burke, A. F. and Bird, K. D., "The Use of Conical and Contcured Expansion Nozzles in Hypervelocity Facilities," Rept. 112, July 1962, Cornell Aeronautical Lab.

[24] Eckert, E. R. G., "Survey on Heat Transfer at High Speeds," WADC-TR-54-70, April 1954, Wright Air Development Center.

[25] Petrie, S. L., "Boundary Layer Studies in an Arc-Heated Wind Tunnel," Research Foundation Rept. 2033, April 1968, The Ohio State Univ.